EXTENDED DATA FIGURES

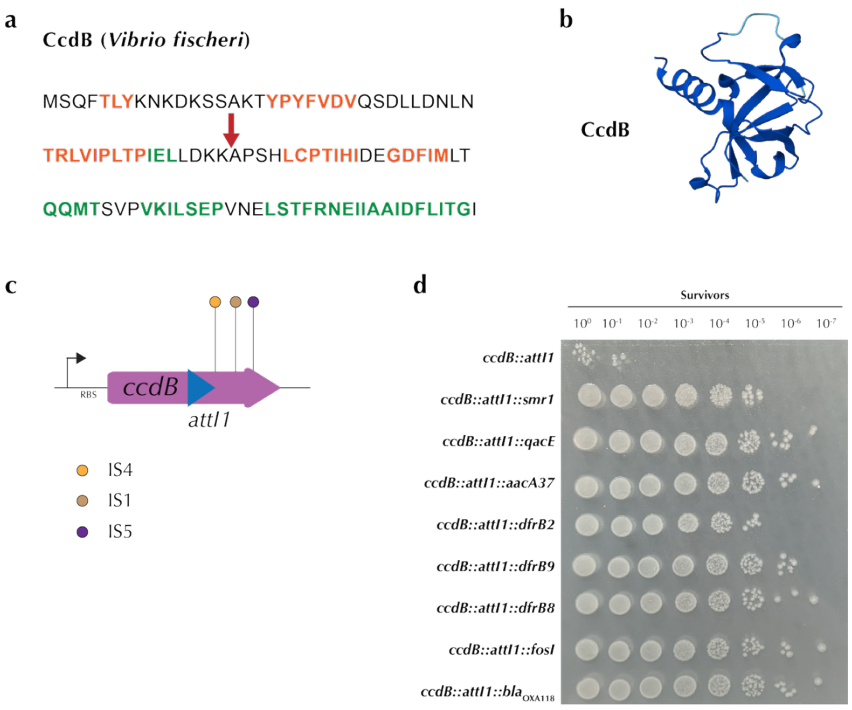

Extended Data Figure 1. a) Chosen location to introduce the *attI1* site in *ccdB* from *Vibrio fischeri*. Orange represents β-sheets and green represents α-helices. These features were predicted using Phyre2. The red arrow illustrates the locations where the *attI1* site was introduced. **b)** Predicted structure of wild-type CcdB protein from *V. fischeri*. Models were generated using AlphaFold3[42]; the blue-to-red scale indicates high to low confidence in folding prediction. pTM = 0.9. **c)** Schematic representation of the escape mutants encountered in the killing assays of *ccdB::attI1*. Colonies were amplified by PCR and mutations identified by Sanger-sequencing (n=30). **d)** Killing assays of *ccdB::attI1::cassette*. The *E. coli* strains contain the various plasmidic constructs mimicking the outcome of a recombination event. These strains were plated in 5 µL spots in dilutions up to 10^{-7}, in killing conditions.

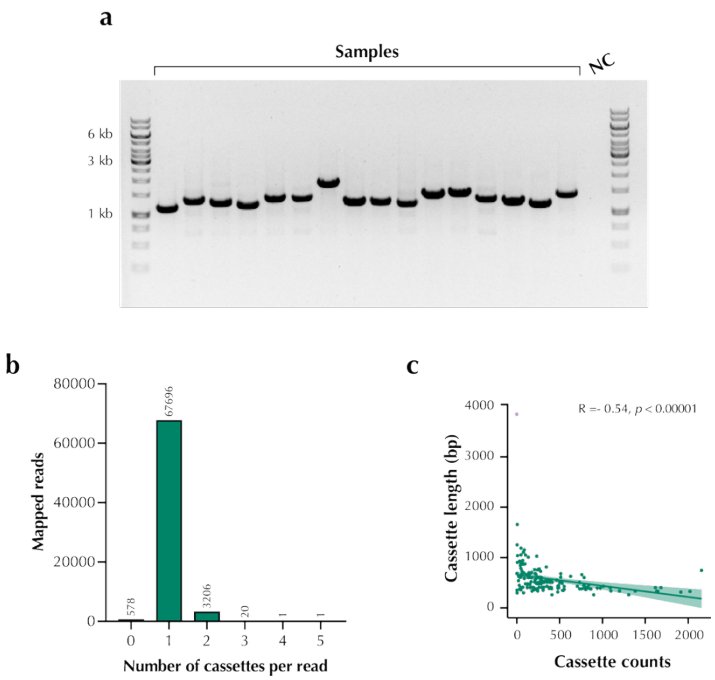

Extended Data Figure 2. a) Example of a colony PCR result of the captured cassettes in the plasmid vector. The expected size of the empty *ccdB::attI1* would be 667 bp. NC, PCR negative control. **b)** Number of reads that mapped to 0-5 cassettes. **c)** Correlation of the cassette length and the number of counts of the same cassette. Spearman R and *p*-value are shown.

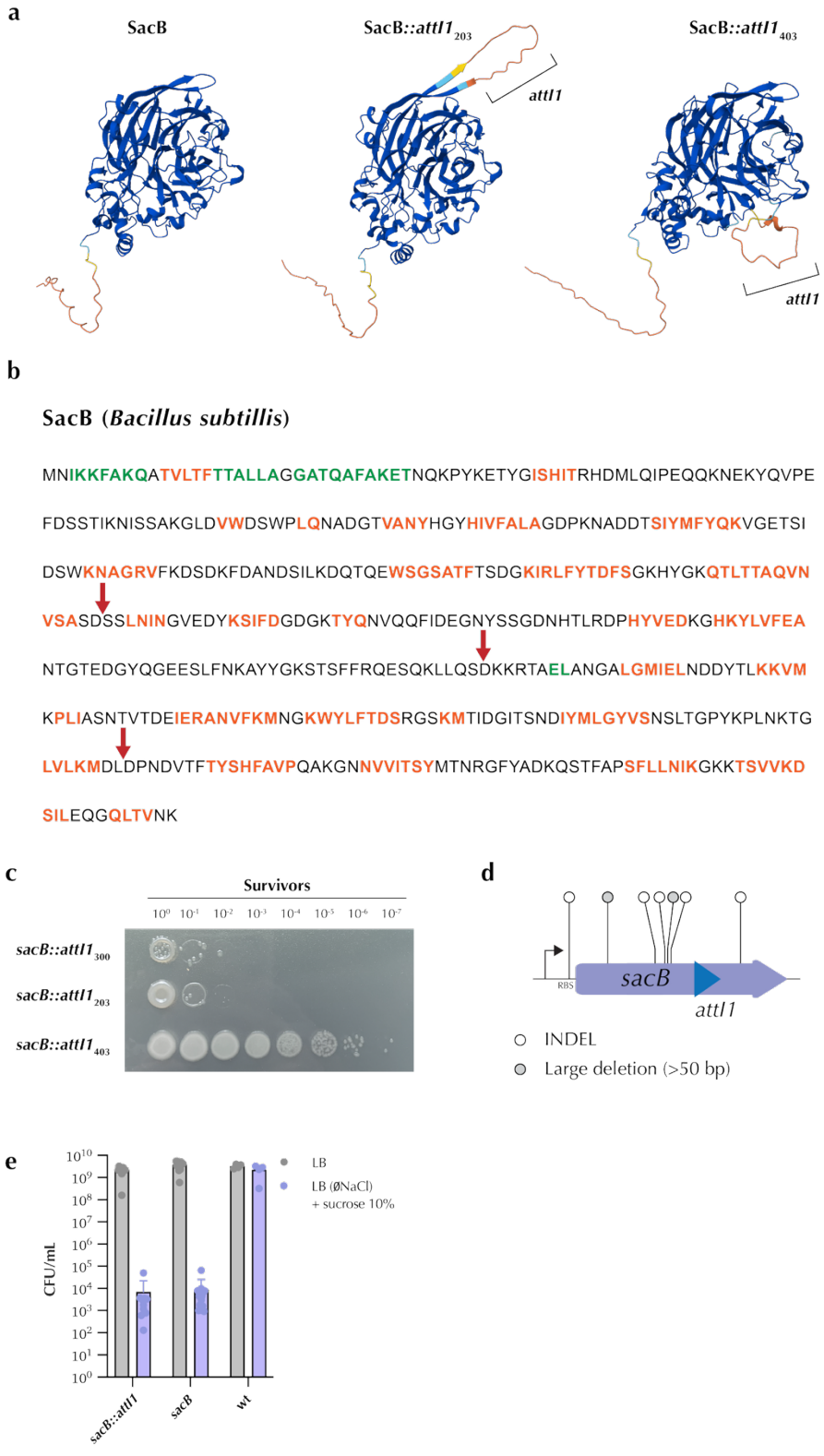

Extended Data Figure 3. a) Predicted structures of wild-type SacB protein from *Bacillus subtilis* and SacB::*attI1*$_{203}$ and SacB::*attI1*$_{403}$, highlighting the integration *attI1* site and altered folding. Models were generated using AlphaFold3[42], blue-to-red scale indicates high to low confidence in folding prediction. pTM = 0.92, 0.9, and 0.89, respectively. **b)** Chosen locations

to introduce the *attI1* site in *sacB* from *B. subtilis*. Orange represents β-sheets and green represents α-helices. These features were predicted using Phyre2. Red arrows illustrate the locations where the *attI1* site was introduced. **c)** Survivors in a killing assay testing the three SacB::*attI1* versions. The three constructs were plated in 5µL spots in dilutions up to 10^{-7}, in killing conditions in LB (ØNaCl) + sucrose 10%. **d)** Schematic representation of the escape mutants encountered in the killing assays of *sacB::attI1*. Colonies were amplified by PCR and mutations identified by Sanger-sequencing (n=10). **e)** Cell counts of the killing assays of the *sacB*-based platform cloned in *V. cholerae* N16961 ΔSI compared to the WT gene. The WT strain (*sacB* free) was used as a control for growth in the different tested media. Cells were grown in either survival conditions (standard LB medium) or killing conditions (LB (ØNaCl) + sucrose 10%).

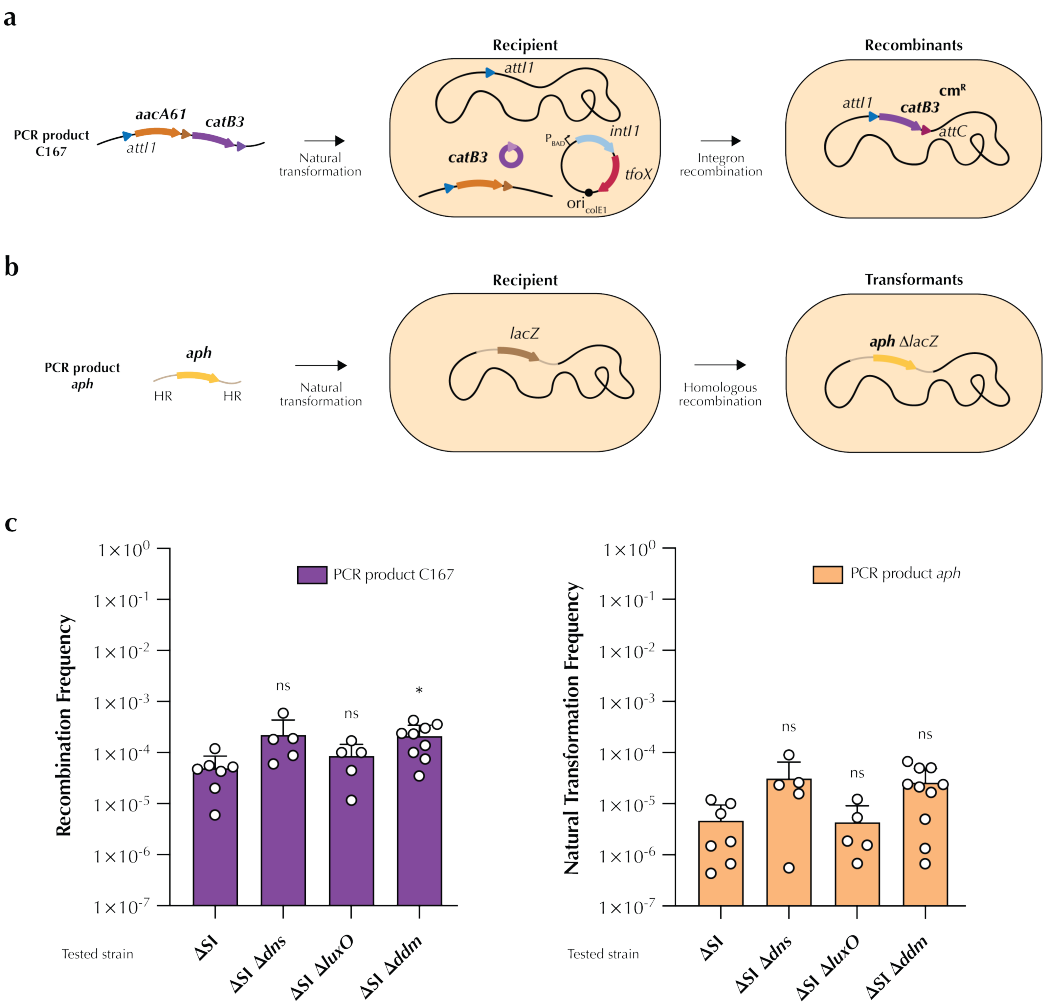

Extended Data Figure 4. a) Schematic representation of the recombination assay. Recipient cells were transformed with a PCR-amplified integron array upon arabinose-mediated *tfoX* and *intI1* induction. The different *V. cholerae* ΔSI Δ*ddm* mutants contain an *attI1* site in the chromosome. The capture of the second cassette (*catB3*) was selected by phenotype, i.e., chloramphenicol resistance. **b)** Schematic representation of the classical natural transformation assay. Above, a *V. cholerae* recipient is depicted with the *lacZ* gene and its adjacent regions. The transforming DNA corresponds to a kanamycin resistance gene (*aph*) and its promoter, flanked by adjacent regions of the target (in light brown), called homology regions (HR). After transformation, the *aph* gene substitutes the *lacZ* gene by homologous recombination, allowing for the selection of transformants. **c)** Recombination and transformation frequencies are given on the Y-axis and were calculated as the ratio of the number of CFUs resistant to chloramphenicol or kanamycin versus the total number of CFUs. Bar charts show the mean of the recombination/transformation frequency ± s.d. from several biological replicates (individual dots). Statistical significance between each mutant and the ΔSI control was determined using the Kruskal-Wallis test with Dunnett's correction for multiple comparisons; ns, not significant, *, $p < 0.05$.

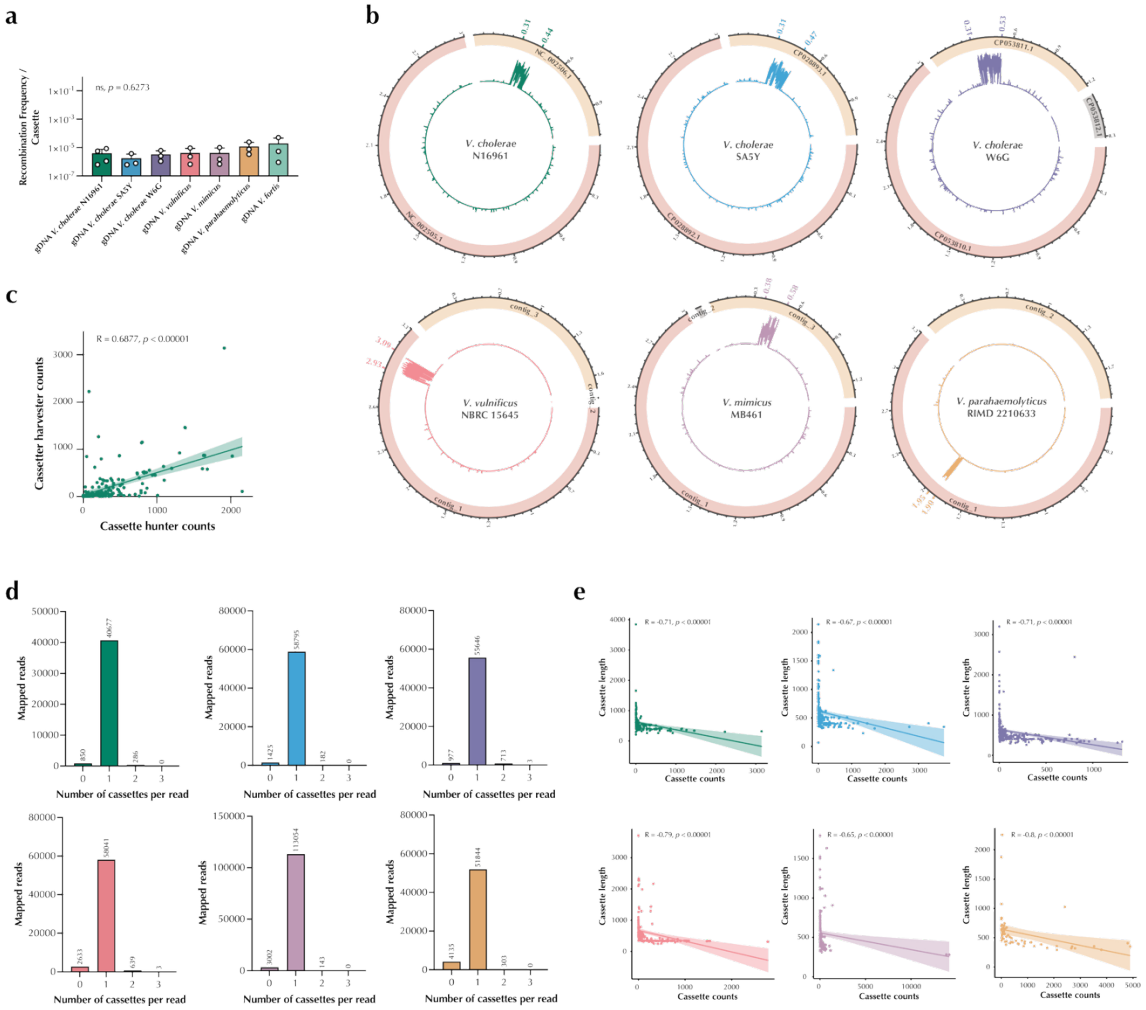

Extended Data Figure 5. a) Recombination frequency per cassette of each genomic sample tested. Statistical significance between samples was determined using the Kruskal-Wallis test with Dunnett's correction for multiple comparisons; ns, not significant. **b)** Average coverage per kilobase (colored plots) given in log10 reads of the contigs of each *Vibrio* spp. genome. SCI positions are highlighted in bold. **c)** Correlation between the cassette counts retrieved on the cassette gatherer tool and the cassette hunter tool for the *V. cholerae* N16961 SCI. **d)** Number of reads that mapped to 0-5 cassettes. **e)** Correlation of the cassette length and the number of counts of the same cassette for each library generated. Spearman R and p-value are shown.

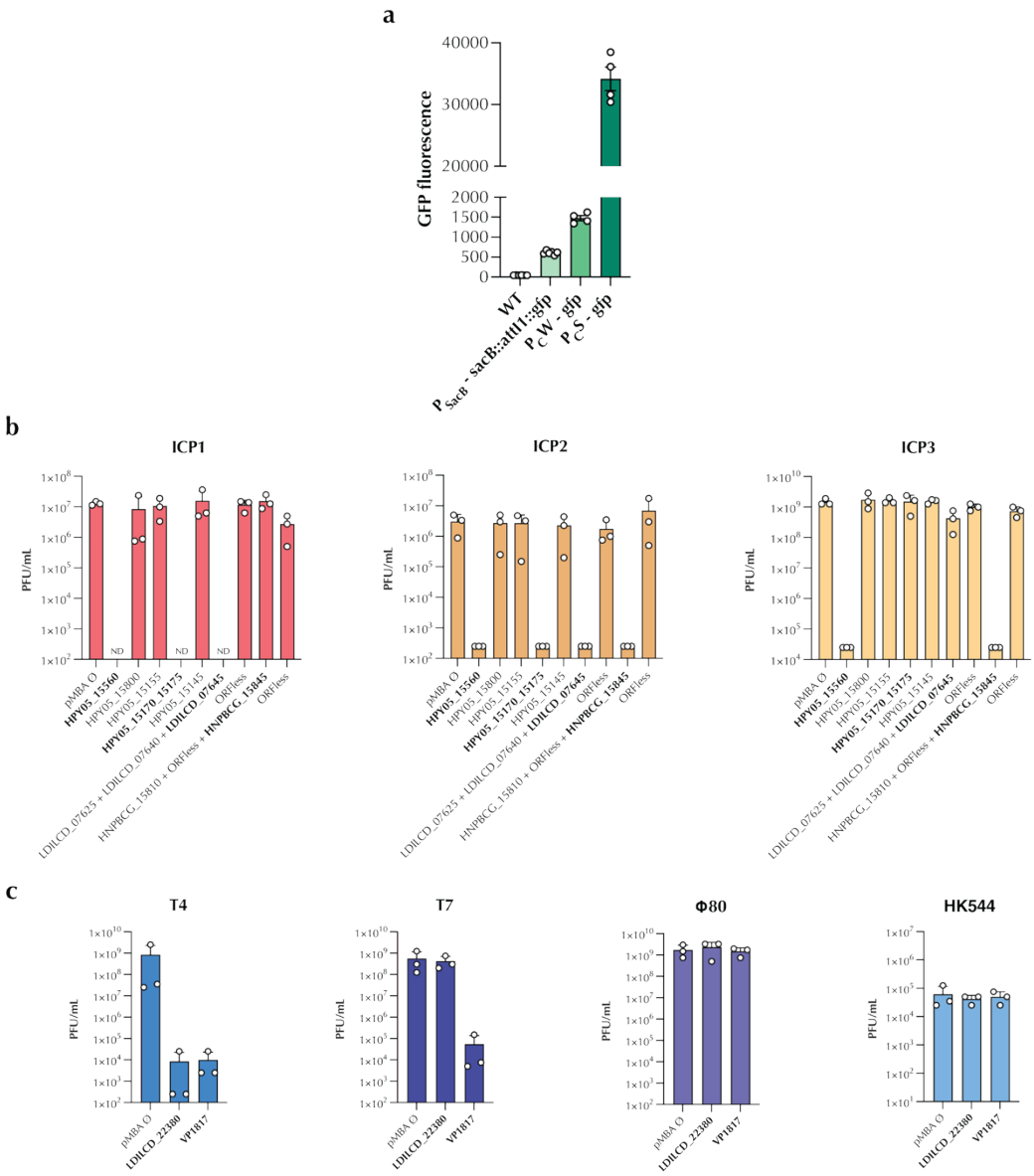

Extended Data Figure 6. a) GFP fluorescence intensity (FITC-A, arbitrary units) measured by flow cytometry of three different promoters controlling the *gfp* gene in *V. cholerae* N16961. WT represents the empty strain, as a no-fluorescent control. Dots represent biological replicates. **b)** Plaque-forming units (PFU) per mL of tested integron cassettes against Vibriophages ICP1, ICP2, and ICP3. **c)** Plate-forming units (PFU) per mL of tested integron cassettes against *E. coli* phages T4, T7, Φ80, and HK544.